Chimeras in random non-complete networks of phase oscillators

Carlo R. Laing*
Institute of Information and Mathematical Sciences, Massey University, Private Bag 102-904 NSMC, Auckland, New Zealand

Karthikeyan Rajendran
Department of Chemical and Biological Engineering, Princeton University, Princeton, New Jersey 08544, USA

Ioannis G. Kevrekidis
Department of Chemical and Biological Engineering and Program in Applied and Computational Mathematics (PACM), Princeton University, Princeton, New Jersey 08544, USA

(Dated: February 24, 2012)

We consider the simplest network of coupled non-identical phase oscillators capable of displaying a "chimera" state (namely, two subnetworks with strong coupling within the subnetworks and weaker coupling between them) and systematically investigate the effects of gradually removing connections within the network, in a random but systematically specified way. We average over ensembles of networks with the same random connectivity but different intrinsic oscillator frequencies and derive ODEs whose fixed points describe a typical chimera state in a representative network of phase oscillators. Following these fixed points as parameters are varied we find that chimera states are quite sensitive to such random removals of connections, and that oscillations of chimera states can be either created or supressed in apparent bifurcation points, depending on exactly how the connections are gradually removed.

PACS numbers: 05.45.Xt
Keywords: chimera states, coupled oscillators, bifurcation

Chimera states are known to occur in networks of identical phase oscillators and are characterised by some fraction of the oscillators being synchronised while the remainder are asynchronous. Previous studies of these states have considered highly symmetric networks, with all-to-all connectivity. The question as to the robustness of these states with respect to changes in the network structure naturally arises. Here we systematically investigate this issue for what is arguably the simplest network that shows chimera states, considering two different systematic ways of perturbing an all-to-all connected network. By varying parameters controlling the oscillators' dynamics, as well as parameters controlling the topology of the network, we can determine the effects of changing this topology on the existence and stability of chimera states. We find that chimera states are quite sensitive to changes in the network topology, and that one of the perturbations considered supresses oscillations of chimera states, while the other promotes oscillations.

I. INTRODUCTION

Networks of coupled oscillators have been studied for many years, with the Kuramoto model of phase oscillators being one of the most studied [1–10]. In these models, the state of oscillator i is given by the angular variable θ_i, and oscillators are coupled to one another through sinusoidal functions of phase differences. Much effort has gone into characterising the influence of coupling strength and oscillators' intrinsic frequencies on oscillator synchronisation [4, 5, 8, 10]. However, in the last decade or so a number of researchers have studied an interesting phenomenon referred to as a "chimera" state, observed in highly-symmetric networks of identical phase oscillators [1, 7, 11–16]. This state is one in which — although the oscillators are identical — some fraction of them are synchronous while the remainder are asynchronous. One of the simplest systems used to study this phenomenon is a network formed from two identical sub-networks, with strong all-to-all coupling within sub-networks and weaker all-to-all coupling between subnetworks. Such a system was studied by Abrams et al. [7], who used the ansatz of Ott and Antonsen [17–19] to show that this

*Electronic address: c.r.laing@massey.ac.nz

system, in the limit of an infinite number of oscillators, could be described by three ordinary differential equations. However, Pikovsky and Rosenblum [20] showed, using the ansatz of Watanabe and Strogatz [21], that the Ott/Antonsen (OA) ansatz did not completely describe the dynamics of such a system when the oscillators were *identical*. Subsequently, Laing [3] studied the same network but with non-identical oscillators, for which the OA ansatz does correctly predict the dynamics. A later study [22] of planar (rather than phase) oscillators coupled as above showed that chimera states are robust with respect to variation of the oscillator amplitude, at least for this type of network. A number of other authors have considered similar pairs of networks of oscillators [23–25].

All previous analyses of chimera states have considered highly structured networks, with either all–to–all coupling within and between subnetworks (but with different strengths within and between subnetworks) [3, 7, 15, 22], or networks with physical spatial structure in which the coupling strength between oscillators depends on only the distance between oscillators [1, 11–13, 16]. Such precisely coupled networks are unlikely to exist in nature, so it is of interest to investigate the robustness of chimera states with respect to changes in the network structure, defined by the coupling between oscillators. This is the question we address here. We use techniques presented in Barlev et al. [8] to study an *ensemble* of networks, each of which has the same structure, namely a fixed perturbation from the case discussed above (a network formed from two statistically identical sub-networks, with all-to-all coupling both between and within sub-networks). For each ensemble member, the set of intrinsic frequencies of the oscillators is chosen randomly and independently from a given distribution, i.e. we consider the case of nonidentical oscillators. By averaging over the ensemble we obtain a set of $2N$ ODEs, where N is the number of oscillators in each subnetwork. The fixed points of these ODEs (when they exist) can be followed as parameters are varied, giving *typical* behaviour of a network of phase oscillators *with the same specified connectivity.*

We consider systematic perturbations of network topology, and by considering a number of different ensembles, each of which is chosen from the *same* family of perturbed networks, we can determine overall trends in the behaviour of such networks as they move away from the highly-symmetric (all-to-all coupled) case. We choose two different parametrised families of network topologies, both of which asymptote in particular limits to the all-to-all coupled case. By varying both the parameters governing the topology of the network and other natural parameters in the system, we can systematically determine the effects of varying the network structure on the existence and stability of chimera states.

We present the model and analyse it in Sec. II, using the techniques of Barlev et al. [8] to average over an ensemble of networks and obtain equations describing the statistics of the corresponding phase oscillator networks. Our results are given in Sec. III, where we first consider the all-to-all coupled case, and then investigate two parametrised families of increasingly sparse networks. We conclude with a discussion in Sec. IV.

II. MODEL AND ANALYSIS

Our system consists of two populations of non-identical phase oscillators, with coupling both between and within populations, but of different respective strengths. The governing equations are

$$\frac{d\theta_j^1}{dt} = \omega_j^1 + \frac{\mu}{N}\sum_{k=1}^{N} A_{jk}\sin\left(\theta_k^1 - \theta_j^1 - \alpha\right) + \frac{\nu}{N}\sum_{k=1}^{N} B_{jk}\sin\left(\theta_k^2 - \theta_j^1 - \alpha\right) \quad (1)$$

$$\frac{d\theta_j^2}{dt} = \omega_j^2 + \frac{\mu}{N}\sum_{k=1}^{N} C_{jk}\sin\left(\theta_k^2 - \theta_j^2 - \alpha\right) + \frac{\nu}{N}\sum_{k=1}^{N} D_{jk}\sin\left(\theta_k^1 - \theta_j^2 - \alpha\right) \quad (2)$$

for $j = 1, \ldots N$, where N is the number of oscillators in each population (subnetwork). The two populations are labelled 1 and 2, with connectivity within population 1 given by the matrix A_{jk}, from population 2 to 1 by B_{jk}, within population 2 by C_{jk} and from 1 to 2 by D_{jk}. The entries of these matrices are either constant (the same constant within each matrix) or 0. The superscripts on the angles label the population to which they belong; the ω_j are all taken from a distribution $g(\omega)$; and μ and ν are given by $\mu = (1+E)/2, \nu = (1-E)/2$, where E is a parameter, as in [3, 7].

If the connectivity matrices are full, i.e. all entries are 1, the system reverts to that studied by Abrams et al. [7] if $g(\omega)$ is a delta function, and to that by Laing [3] (and earlier, by Montbrió et al. [9]) if $g(\omega)$ is a Lorentzian. These authors studied the effects of varying α, E, and the width of the distribution of intrinsic frequencies, $g(\omega)$. (The mean of g can be set to zero by going to a rotating coordinate frame.) Here, instead, we are interested in the combined effects of systematically varying the connectivity matrices $A, \ldots D$, *and*

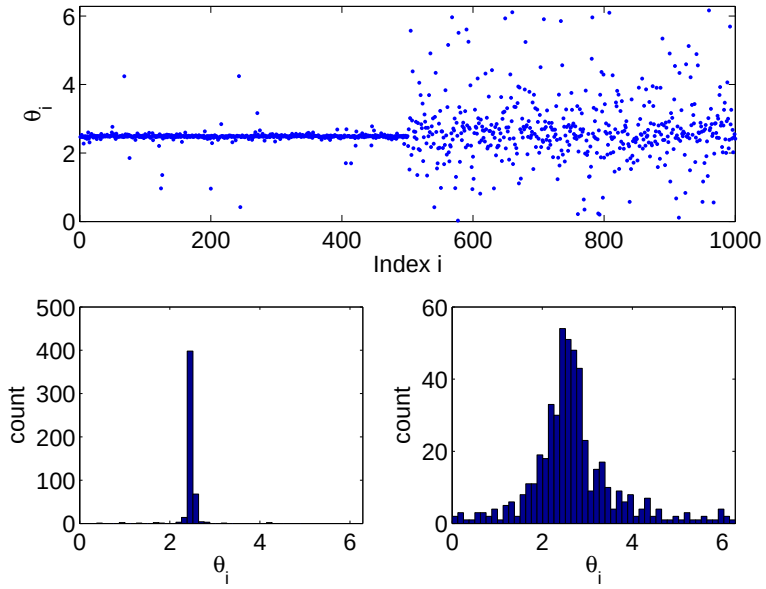

FIG. 1: A chimera solution of (1)-(2) for full connectivity matrices. Top: a temporal snapshot of the phase θ_i as a function of index, i, where those in population 1 are numbered 1 to 500, and those in population 2 are numbered 501 to 1000. Bottom left: histogram of oscillator phases in population 1. Bottom right: histogram of oscillator phases in population 2. Parameter values: $N = 500, E = 0.2, \alpha = \pi/2 - 0.05$. All ω_j chosen from a Lorentzian distribution with half-width-at-half-maximum 0.001.

varying the parameters just mentioned. As an illustration, Fig. 1 shows an example of a chimera state for (1)-(2) when the matrices $A, \ldots D$ are full. We see that in population 1 the oscillators are tightly synchronised, whereas in population 2 they are significantly more asynchronous.

We now use the results of Barlev et al. [8] to derive $2N$ ODEs which describe an ensemble of networks all having the *same* connectivity, but with different realisations of the ω_j in different members of the ensemble. The advantage of this is that the fixed points of these ODEs describe, *on a statistical level*, some of the typical behaviour seen in a realisation of the phase oscillator network with the same connectivity. (The states we are interested in, chimera states, do not correspond to actual fixed points of the phase oscillator system (1)-(2).) These fixed points, which represent on a statistical level typical behaviour which is sampled by a realisation of the phase oscillator network, can then be followed as parameters are varied, and any bifurcations found will lead to insight into the possible representative behaviour of a corresponding phase oscillator network with the same connectivity. By doing this for many different random network structures that are generated in the same systematic way (i.e. that are statistically the same) we can examine the effects of randomly changing, in a prescribed way, connectivity matrices in the above network. By considering different random network structures that are statistically the same, we are effectively averaging over both the intrinsic frequencies of the oscillators, and different realisations of these networks.

First we define four N-dimensional vectors whose jth entries are

$$\widehat{A}_j \equiv \frac{1}{N}\sum_{k=1}^{N} A_{jk}\exp\left(i\theta_k^1\right) \qquad \widehat{B}_j \equiv \frac{1}{N}\sum_{k=1}^{N} B_{jk}\exp\left(i\theta_k^2\right) \tag{3}$$

$$\widehat{C}_j \equiv \frac{1}{N}\sum_{k=1}^{N} C_{jk}\exp\left(i\theta_k^2\right) \qquad \widehat{D}_j \equiv \frac{1}{N}\sum_{k=1}^{N} D_{jk}\exp\left(i\theta_k^1\right) \tag{4}$$

which allows us to write (1)-(2) as

$$\frac{d\theta_j^1}{dt} = \omega_j^1 + \mu\,\mathrm{Im}\left[\widehat{A}_j\exp\left(-i\theta_j^1\right)\exp\left(-i\alpha\right)\right] + \nu\,\mathrm{Im}\left[\widehat{B}_j\exp\left(-i\theta_j^1\right)\exp\left(-i\alpha\right)\right] \tag{5}$$

$$\frac{d\theta_j^2}{dt} = \omega_j^2 + \mu\,\mathrm{Im}\left[\widehat{C}_j\exp\left(-i\theta_j^2\right)\exp\left(-i\alpha\right)\right] + \nu\,\mathrm{Im}\left[\widehat{D}_j\exp\left(-i\theta_j^2\right)\exp\left(-i\alpha\right)\right] \tag{6}$$

for $j = 1, \ldots N$. Now consider an ensemble of systems of this form, with fixed connectivities (i.e. matrices

A, B, C and D), but where each member of the ensemble has a randomly chosen set of frequencies $\{\omega_j^1\}$ and $\{\omega_j^2\}$ (these both come from the same distribution g, and g is the same for each member of the ensemble). Letting the number of members of the ensemble go to infinity we describe the state of population 1 by the probability density function

$$f^1(\theta_1^1, \theta_2^1, \ldots, \theta_N^1; \omega_1^1, \omega_2^1, \ldots \omega_N^1; t)$$

and population 2 by the function

$$f^2(\theta_1^2, \theta_2^2, \ldots, \theta_N^2; \omega_1^2, \omega_2^2, \ldots \omega_N^2; t)$$

which, by conservation of oscillators [4, 18], satisfy

$$\frac{\partial f^\sigma}{\partial t} + \sum_{j=1}^{N} \frac{\partial}{\partial \theta_j^\sigma}\left[f^\sigma\left(\frac{d\theta_j^\sigma}{dt}\right)\right] = 0 \tag{7}$$

for $\sigma = 1, 2$. In this limit the jth entries of the vectors $\widehat{A}, \widehat{B}, \widehat{C}$ and $\widehat{D}$ are defined by

$$\begin{aligned}
\widehat{A}_j &\equiv \frac{1}{N}\sum_{k=1}^{N} A_{jk} \int \exp(i\theta_k^1) f^1(\{\theta^1\}; \{\omega^1\}; t)\, d^N\omega^1\, d^N\theta^1 \\
&= \frac{1}{N}\sum_{k=1}^{N} A_{jk} \int_{-\infty}^{\infty}\int_0^{2\pi} \exp(i\theta_k^1) f_k^1(\theta_k^1, \omega_k^1, t)\, d\theta_k^1\, d\omega_k^1 \qquad (8)\\
\widehat{B}_j &\equiv \frac{1}{N}\sum_{k=1}^{N} B_{jk} \int \exp(i\theta_k^2) f^2(\{\theta^2\}; \{\omega^2\}; t)\, d^N\omega^2\, d^N\theta^2 \\
&= \frac{1}{N}\sum_{k=1}^{N} B_{jk} \int_{-\infty}^{\infty}\int_0^{2\pi} \exp(i\theta_k^2) f_k^2(\theta_k^2, \omega_k^2, t)\, d\theta_k^2\, d\omega_k^2 \qquad (9)\\
\widehat{C}_j &\equiv \frac{1}{N}\sum_{k=1}^{N} C_{jk} \int \exp(i\theta_k^2) f^2(\{\theta^2\}; \{\omega^2\}; t)\, d^N\omega^2\, d^N\theta^2 \\
&= \frac{1}{N}\sum_{k=1}^{N} C_{jk} \int_{-\infty}^{\infty}\int_0^{2\pi} \exp(i\theta_k^2) f_k^2(\theta_k^2, \omega_k^2, t)\, d\theta_k^2\, d\omega_k^2 \qquad (10)\\
\widehat{D}_j &\equiv \frac{1}{N}\sum_{k=1}^{N} D_{jk} \int \exp(i\theta_k^1) f^1(\{\theta^1\}; \{\omega^1\}; t)\, d^N\omega^1\, d^N\theta^1 \\
&= \frac{1}{N}\sum_{k=1}^{N} D_{jk} \int_{-\infty}^{\infty}\int_0^{2\pi} \exp(i\theta_k^1) f_k^1(\theta_k^1, \omega_k^1, t)\, d\theta_k^1\, d\omega_k^1 \qquad (11)
\end{aligned}$$

where f_k^σ ($k \in \{1, \ldots N\}$) is the marginal distribution for the phase of the kth oscillator defined by

$$f_k^\sigma(\theta_k^\sigma, \omega_k^\sigma, t) = \int f^\sigma(\{\theta^\sigma\}; \{\omega^\sigma\}; t) \prod_{j\neq k} d\omega_j^\sigma\, d\theta_j^\sigma.$$

Note that the vectors $\widehat{A}, \widehat{B}, \widehat{C}$ and $\widehat{D}$ are functions of time only. Multiplying (7) by $\prod_{j\neq k}\, d\omega_j^\sigma\, d\theta_j^\sigma$ and integrating we find that each f_k^σ satisfies

$$\frac{\partial f_k^\sigma}{\partial t} + \frac{\partial}{\partial \theta_k^\sigma}\left[f_k^\sigma\left(\frac{d\theta_k^\sigma}{dt}\right)\right] = 0 \tag{12}$$

The OA ansatz [17–19] is an assumption on the form of the Fourier series in the angular direction for the f_k, namely that

$$f_k^1(\theta_k^1, \omega_k^1, t) = \frac{g(\omega_k^1)}{2\pi}\left[1 + \sum_{n=1}^{\infty} [\alpha_k(\omega_k^1, t)]^n \exp(in\theta_k^1) + c.c.\right] \tag{13}$$

and

$$f_k^2(\theta_k^2,\omega_k^2,t)=\frac{g(\omega_k^2)}{2\pi}\left[1+\sum_{n=1}^{\infty}[\beta_k(\omega_k^2,t)]^n\exp\left(in\theta_k^2\right)+c.c.\right] \tag{14}$$

where "$c.c.$" is the complex conjugate of the previous term and $|\alpha_k|,|\beta_k|\leq 1$ for convergence. Substituting these Fourier series into (12) we find that the α_k and β_k satisfy

$$\frac{d\alpha_k}{dt}=-i\omega_k^1\alpha_k+(e^{i\alpha}/2)\left(\mu\overline{\widehat{A}}_k+\nu\overline{\widehat{B}}_k\right)-(e^{-i\alpha}/2)\left(\mu\widehat{A}_k+\nu\widehat{B}_k\right)\alpha_k^2 \tag{15}$$

and

$$\frac{d\beta_k}{dt}=-i\omega_k^2\beta_k+(e^{i\alpha}/2)\left(\mu\overline{\widehat{C}}_k+\nu\overline{\widehat{C}}_k\right)-(e^{-i\alpha}/2)\left(\mu\widehat{C}_k+\nu\widehat{D}_k\right)\beta_k^2 \tag{16}$$

where overline indicates complex conjugate. Substituting the ansatz (13)-(14) into (8)-(11) we obtain

$$\widehat{A}_j=\frac{1}{N}\sum_{k=1}^{N}A_{jk}\int_{-\infty}^{\infty}\overline{\alpha}_k(\omega_k^1,t)g(\omega_k^1)\,d\omega_k^1 \tag{17}$$

$$\widehat{B}_j=\frac{1}{N}\sum_{k=1}^{N}B_{jk}\int_{-\infty}^{\infty}\overline{\beta}_k(\omega_k^2,t)g(\omega_k^2)\,d\omega_k^2 \tag{18}$$

$$\widehat{C}_j=\frac{1}{N}\sum_{k=1}^{N}C_{jk}\int_{-\infty}^{\infty}\overline{\beta}_k(\omega_k^2,t)g(\omega_k^2)\,d\omega_k^2 \tag{19}$$

$$\widehat{D}_j=\frac{1}{N}\sum_{k=1}^{N}D_{jk}\int_{-\infty}^{\infty}\overline{\alpha}_k(\omega_k^1,t)g(\omega_k^1)\,d\omega_k^1. \tag{20}$$

If

$$g(\omega)=\frac{\Delta/\pi}{\omega^2+\Delta^2}$$

i.e. $g(\omega)$ is a Lorentzian with half-width-at-half-maximum of Δ and centred (without loss of generality) at $\omega=0$, then we obtain (using contour integration [3, 18])

$$\widehat{A}_j=\frac{1}{N}\sum_{k=1}^{N}A_{jk}\overline{\alpha}_k(-i\Delta,t)\qquad\widehat{B}_j=\frac{1}{N}\sum_{k=1}^{N}B_{jk}\overline{\beta}_k(-i\Delta,t) \tag{21}$$

$$\widehat{C}_j=\frac{1}{N}\sum_{k=1}^{N}C_{jk}\overline{\beta}_k(-i\Delta,t)\qquad\widehat{D}_j=\frac{1}{N}\sum_{k=1}^{N}D_{jk}\overline{\alpha}_k(-i\Delta,t) \tag{22}$$

Defining $a_k(t)\equiv\alpha_k(-i\Delta,t)$ and $b_k(t)\equiv\beta_k(-i\Delta,t)$ and evaluating (15)-(16) at $\omega_k^1=\omega_k^2=-i\Delta$ we obtain the $2N$ ODEs

$$\frac{da_k}{dt}=-\Delta a_k+\overline{R}_k-R_ka_k^2 \tag{23}$$

$$\frac{db_k}{dt}=-\Delta b_k+\overline{S}_k-S_kb_k^2 \tag{24}$$

for $k=1,\ldots N$ where

$$R_k=e^{-i\alpha}\left(\mu\widehat{A}_k+\nu\widehat{B}_k\right)/2 \tag{25}$$

$$S_k=e^{-i\alpha}\left(\mu\widehat{C}_k+\nu\widehat{D}_k\right)/2 \tag{26}$$

and

$$\widehat{A}_j = \frac{1}{N}\sum_{k=1}^{N} A_{jk}\overline{a}_k \qquad \widehat{B}_j = \frac{1}{N}\sum_{k=1}^{N} B_{jk}\overline{b}_k \tag{27}$$

$$\widehat{C}_j = \frac{1}{N}\sum_{k=1}^{N} C_{jk}\overline{b}_k \qquad \widehat{D}_j = \frac{1}{N}\sum_{k=1}^{N} D_{jk}\overline{a}_k \tag{28}$$

The interpretation of the a_k is that the magnitude of a_k gives the "peaked-ness" of the angular distribution over the ensemble of the θ_k^1 — the closer $|a_k|$ is to 1 the more peaked the distribution, while $|a_k| = 0$ corresponds to a uniform angular distribution. The argument of a_k gives the phase about which the distribution of the θ_k^1 are peaked. Similarly for the b_k and population 2.

Note that when A, B, C and D are full, there exists a solution of (23)-(28) for which $a_k = a$ and $b_k = b\ \forall k$, where a and b are governed by the two complex equations studied by Laing [3]:

$$\frac{da}{dt} = -\Delta a + (e^{i\alpha}/2)(\mu a + \nu b) - (e^{-i\alpha}/2)(\mu\overline{a} + \nu\overline{b})a^2 \tag{29}$$

$$\frac{db}{dt} = -\Delta b + (e^{i\alpha}/2)(\mu b + \nu a) - (e^{-i\alpha}/2)(\mu\overline{b} + \nu\overline{a})b^2 \tag{30}$$

If $\Delta = 0$, (29)-(30) are the same equations as studied by Abrams et al. [7]. As Barlev et al. [8] noted, this type of sychronised solution, for which $a_k = a$ and $b_k = b\ \forall k$, also exists when the coupling matrices all have the same row sum, i.e. all of the oscillators have the same in–degree. Note that (29)-(30) were derived by Abrams et al. [7] not by averaging over an infinite ensemble of finite networks as done by Barlev et al. [8], but by considering the limit $N \to \infty$ for a single network with full connectivity.

III. RESULTS

We now consider the solutions of (23)-(28). For concreteness we set $\Delta = 0.001$; we also define $\beta = \pi/2 - \alpha$. In order to understand the results for randomly connected networks we first consider the all-to-all coupled case. We then consider increasingly sparsely connected networks where the sparseness is gradually introduced in two different random but systematic ways. Firstly, we randomly remove connections between oscillators, with the same probability of removal for all connections. We then consider randomly removing connections in a preferential way so as to create a specific skewed degree distribution.

A. All-to-all coupling

Firstly, consider the all-to-all coupled case. We are interested in chimera state solutions of (29)-(30). A chimera state is a solution of (29)-(30) for which $|a|$ is very close to 1 with $|b|$ significantly less than 1, or vice versa. (If $\Delta = 0$, the chimera state would have $|a|$ exactly equal to 1.) The interpretation of this solution is that oscillators in population 1 are tightly "clustered" in phase, while those in population 2 are significantly less clustered, as seen in Fig. 1. There is also a constant phase difference between the most likely phases of the oscillators in the two populations. For the same parameters as used in Fig. 1 numerical calculations show that the chimera solution of (29)-(30) has $|a| = 0.98573$ and $|b| = 0.68862$ with a phase difference between a and b of 0.095742 (compare with Fig. 1).

Following this chimera state as β is varied we obtain Fig. 2. We see that as β is increased the stable chimera is destroyed in a saddle-node bifurcation, and when β is decreased it dies in a pitchfork bifurcation involving the symmetric state in which $|a| = |b|$. Following these bifurcations as both E and β are varied we obtain Fig. 3. (Recall that E is the strength of the "within subnetwork" coupling relative to the "between subnetwork" coupling, and β is related to the phase offset in (1)-(2).) We see that for moderately small E and β a stable chimera exists. As β is increased the chimera is destroyed in a saddle-node bifurcation, and as E is increased it undergoes a Hopf bifurcation. Although we will only consider $\Delta = 0.001$ in the rest of this paper, Fig. 4 shows how some of the curves in Fig. 3 move as Δ is varied. We only show the curves which bound the region of parameter space in which a stable chimera exists, and see that increasing Δ, i.e. making the oscillators more heterogeneous, causes the left-most pitchfork bifurcation to move to higher β, the Hopf bifurcation to move to higher E, and the saddle-node bifurcation to move very little. Figure 4 should be compared with Fig. 4 in [7], where the authors analyse chimera states when $\Delta = 0$, i.e. the oscillators are identical.

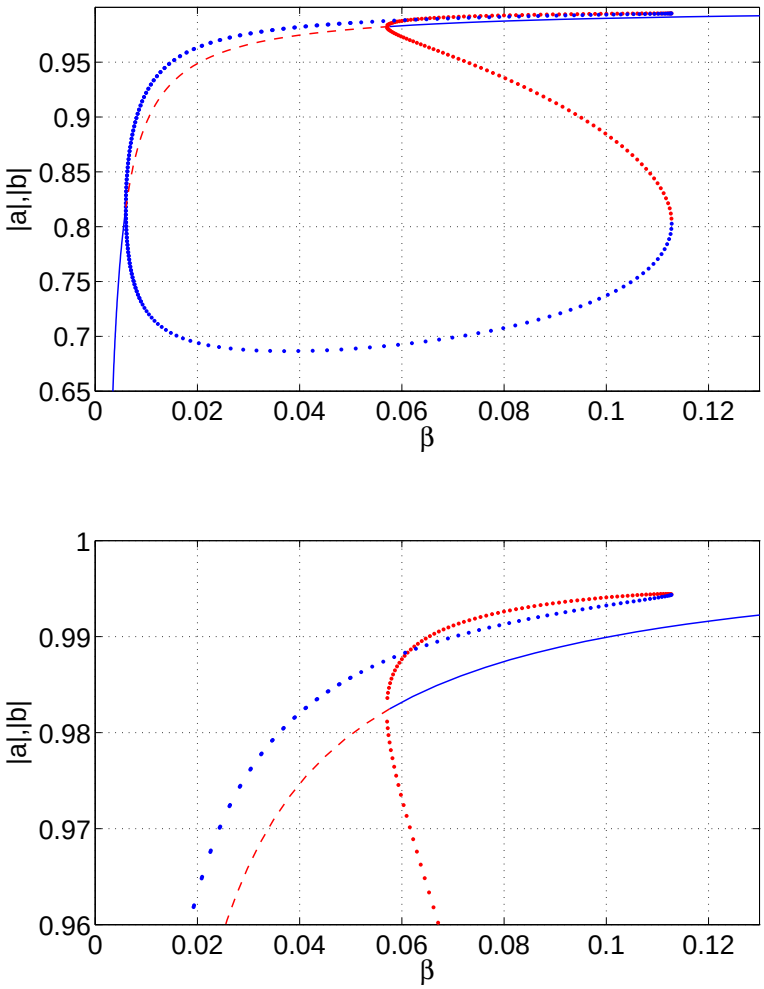

FIG. 2: (color online) Steady states of (29)-(30), where $\beta = \pi/2 - \alpha$. This figure relates to the all-to-all coupled case in the limit $N \to \infty$. Lines indicate symmetric solutions for which $|a| = |b|$; solid blue: stable, dashed red: unstable. Points indicate chimera states where $|a| \neq |b|$; blue: stable, red: unstable. The symmetric state undergoes two pitchfork bifurcations as β is varied. The lower panel is an enlargement of the upper panel. Parameters: $E = 0.2, \Delta = 0.001$.

B. "Sparse" coupling matrices

We now return to the system (23)-(28). As noted by others [2, 12], in order to find steady states of equations like (23)-(24) we must move to a rotating coordinate frame. Thus we replace (23)-(24) by

$$\frac{da_k}{dt} = (i\Omega - \Delta)a_k + \overline{R}_k - R_k a_k^2 \tag{31}$$

$$\frac{db_k}{dt} = (i\Omega - \Delta)b_k + \overline{S}_k - S_k b_k^2 \tag{32}$$

where Ω is the (as yet unknown) rotation frequency. Steady states of (31)-(32) and (25)-(28) are invariant under a rotation $a_k \mapsto a_k e^{i\gamma}$ and $b_k \mapsto b_k e^{i\gamma}$ for any $\gamma \in \mathbb{R}$, reflecting the invariance of the network (1)-(2) under uniform phase shifts applied to each oscillator. We remove this degeneracy by "pinning" the phase of one of the a_k; this extra condition then allows us to find Ω. We first consider increasing β for $E = 0.2$. From Fig. 3 we see that for full connectivity matrices this will lead to the destruction of a chimera through a saddle-node bifurcation, and we are now interested in what happens as β is increased for "sparse" connectivity matrices. (For convenience, we use the term "sparse" below to refer to connectivity matrices that are not full. As we will see, they are not actually sparse in the usual sense of having a majority of zero entries.) We set $N = 300$ and consider several different systematic ways of perturbing away from the case of full connectivity.

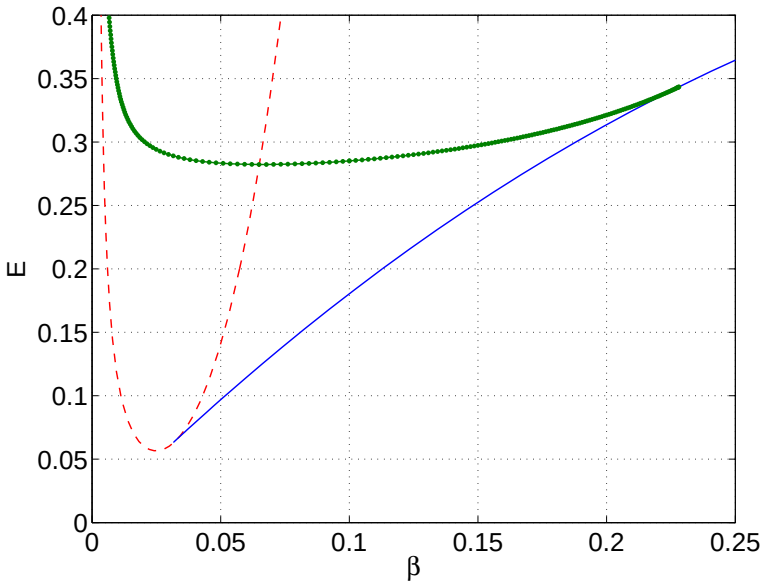

FIG. 3: (color online) Bifurcations of fixed points of (29)-(30). Green dots: Hopf bifurcation of the stable chimera; blue line: saddle-node bifurcation of the stable and unstable chimera; red dotted: pitchfork bifurcation of the symmetric state in which $|a| = |b|$. A stable chimera exists in the region bounded by the left-most pitchfork bifurcation, the saddle-node bifurcation and the Hopf bifurcation. Figure 2 is a horizontal "slice" through this Figure at $E = 0.2$. Parameter: $\Delta = 0.001$.

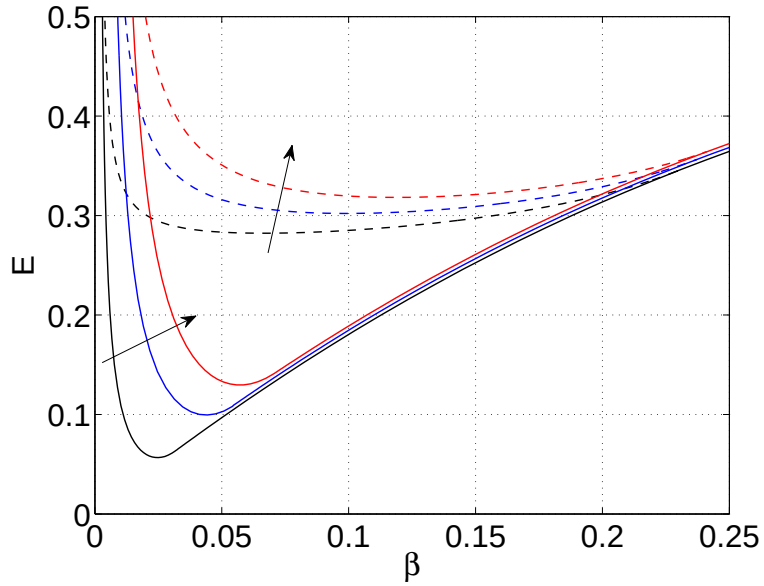

FIG. 4: (color online) Hopf (dashed) and saddle-node and left-most pitchfork (solid) bifurcations of fixed points of (29)-(30) for $\Delta = 0.001$ (black, also shown in Fig. 3), $\Delta = 0.003$ (blue) and $\Delta = 0.005$ (red). The arrows indicate how the curves move as Δ is increased. A stable chimera exists within the region bounded by curves of the same colour, for the corresponding value of Δ.

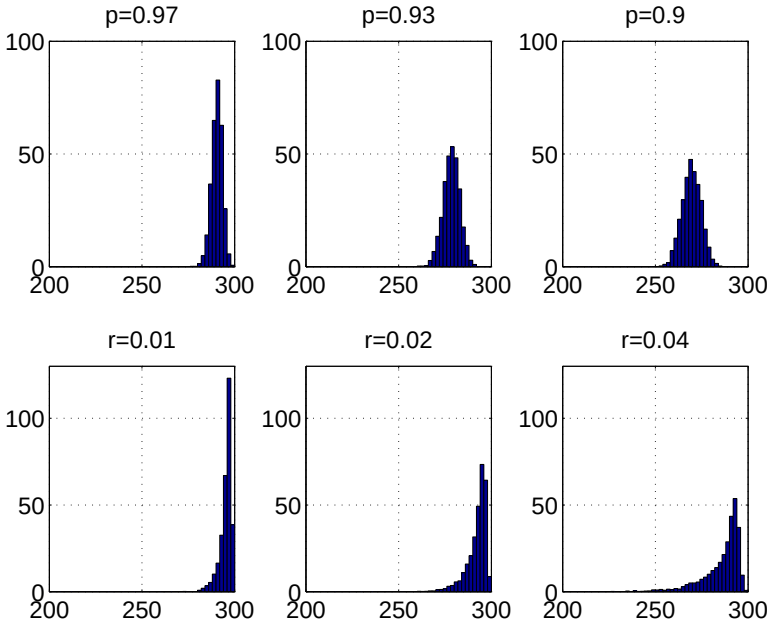

FIG. 5: Degree distributions for Erdös-Rényi-type networks (top row) and Chung-Lu-type networks (bottom row). See text for explanation of parameters. Here $N = 300$.

1. *Erdös-Rényi type networks*

In our first example we consider randomly deleting entries from the matrices A, B, C and D, and increasing the remaining values of the weights to compensate. More precisely, for the matrix A we choose

$$A_{ij} = \begin{cases} 1/p, & \text{with probability } p \\ 0, & \text{with probability } 1-p \end{cases}$$

for all $1 \leq i, j \leq N$ where $0 < p \leq 1$. Thus $p = 1$ corresponds to A being full. If A is thought of as the adjacency matrix of a graph, the constructed matrix corresponds to a weighted (with equal weights) directed Erdös-Rényi (ER) graph, where p is the probability that any one of the N^2 connections from oscillator j to oscillator i exists. Note that we do not normalise the sum of all of the entries of A to be N^2, but the expected value of this sum is N^2, due to the weighting of connections. We construct the matrices B, C and D in the same way. Typical degree distributions (i.e. histograms of the number of oscillators connected to a particular oscillator) for three different values of p are shown in Fig. 5 (top row).

An example of a stable chimera state for the ensemble ODEs (i.e. a stable fixed point of (31)-(32) and (25)-(28)) when $p = 0.97$ is shown in Fig. 6 (top two panels), where population 1 is partially coherent and population 2 is largely synchronised, as indicated by the magnitudes of the a_i and b_i. This Figure also shows (in the bottom panel) a snapshot of the corresponding chimera state in the phase oscillator network (1)-(2). If we follow a fixed point of (25)-(28) and (31)-(32) as β is increased, by referring to Fig. 3 we expect the stable solution to be destroyed in a saddle-node bifurcation. This does happen, and recording the value of β at which this occurs (β_{sn}) for a number of different realisations of the networks and different values of p, we obtain Fig. 7. We see that the chimera state is destroyed at a smaller value of β than the value corresponding to the case of full connectivity, and that these values decrease as p is decreased, i.e. as the networks are made more sparse. We repeated these calculations with $N = 100$ and found that smaller networks were more sensitive to the removal of connections. That is, for $N = 100$ and the values of p used in Fig. 7, the saddle-node bifurcations occurred at even lower values of β than those shown in Fig. 7 for $N = 300$ (results not shown).

Setting B and D to be full while keeping A and C sparse, viz. the case where there are sparse connections only within populations, not between them, gives results very similar to those in Fig. 7. However, if A and C full and B and D are sparse, i.e. there are sparse connections only between populations, this makes the system more robust in the sense that (in this case) for the same values of p, the curve of saddle-node bifurcations seen in Fig. 7 does not move down so much (not shown). Referring to Fig. 3, the interpretation

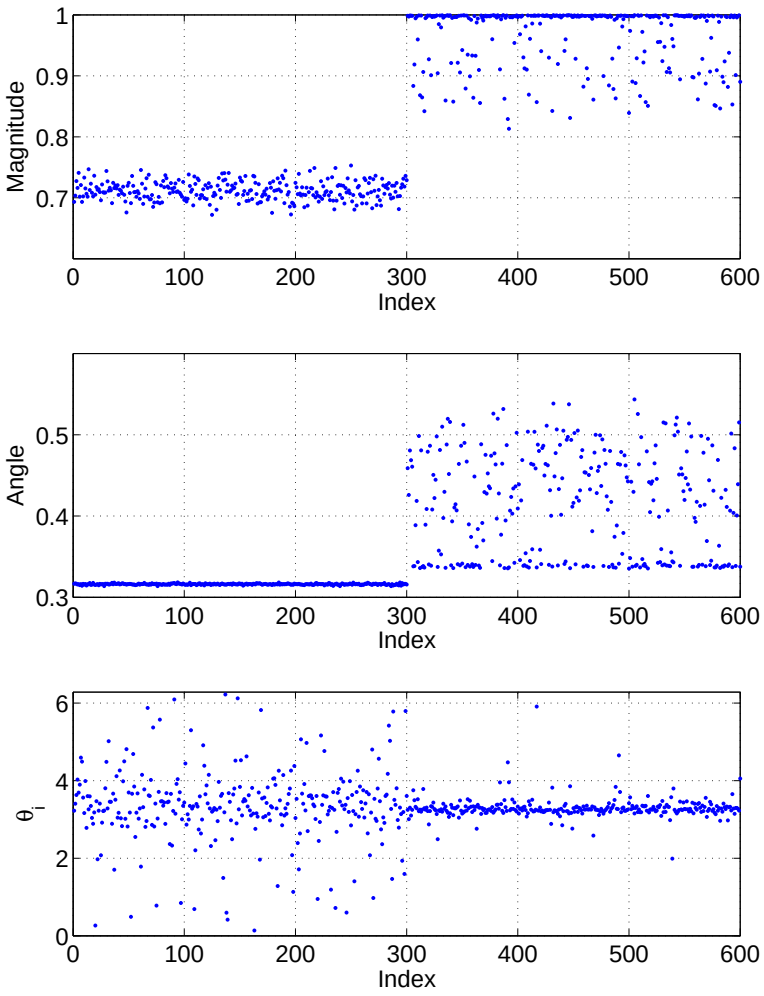

FIG. 6: A chimera solution in a network with Erdös-Rényi-type connectivity. Oscillators in population 1 are numbered 1 to 300, those in population 2 are numbered 301 to 600. Top and middle panels show fixed points of (31)-(32), while the bottom panel is a snapshot of (1)-(2) for the same connectivity matrices. Top: magnitudes of the a_i (left) and b_i (right). Middle: argument of the a_i (left) and b_i (right). Other parameters: $N = 300, p = 0.97, E = 0.2, \Delta = 0.001, \beta = 0.05$.

of these results is that modifying the network in this way decreases the size of the (E, β) parameter space in which a stable chimera exists.

Now consider holding $\beta = 0.05$ and increasing E. We see from Fig. 3 that when the coupling matrices are full this results in a Hopf bifurcation of the chimera state. The results of doing this for the modified networks and various values of p are shown in Fig. 8. We see a similar trend as for the saddle-node bifurcation: removing more and more connections in this way decreases the value of the parameter at which a stable chimera undergoes a bifurcation, again shrinking the size of the parameter space in which a stable chimera exists. Figure 8 suggests something perhaps surprising: if we hold E at say 0.26, a system with full connectivity will support a stable chimera, but if we decrease p to 0.9, the chimera should (with high probability) undergo a Hopf bifurcation. We show an example of this in Fig. 9 for the full oscillator network (1)-(2), where we abruptly switch the connectivity matrices from full to sparse ($p = 0.9$). As predicted, we see the onset of coherent oscillations. The type of simulation shown in Fig. 9 was repeated for a number of different realisations of the ω_i and different connectivity matrices, and the results were always qualitatively the same.

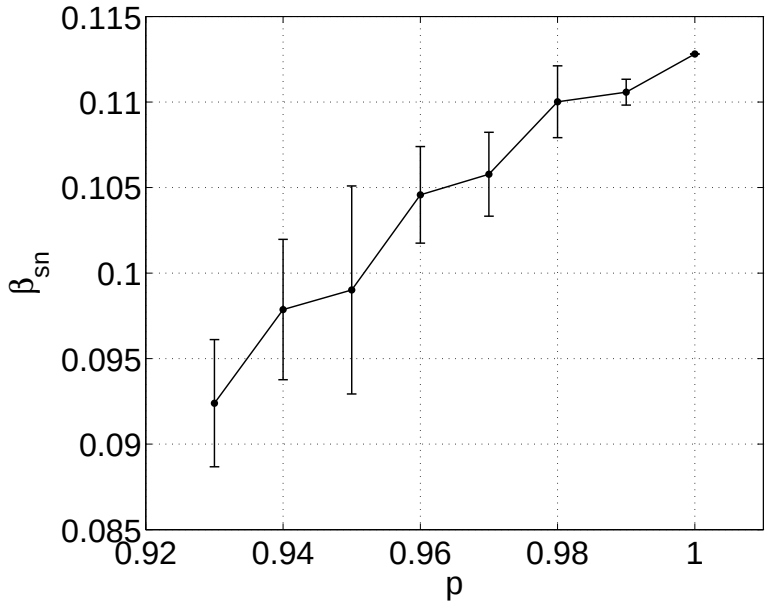

FIG. 7: The values of β_{sn} for which there is a saddle-node bifurcation of fixed points of (25)-(28) and (31)-(32) for Erdös-Rényi-type random matrices A, B, C and D, as a function of p. At each value of p, 10 realisations of the random matrices were used, and the mean and standard deviation of the 10 β_{sn} are shown. Other parameters: $N = 300, E = 0.2, \Delta = 0.001$.

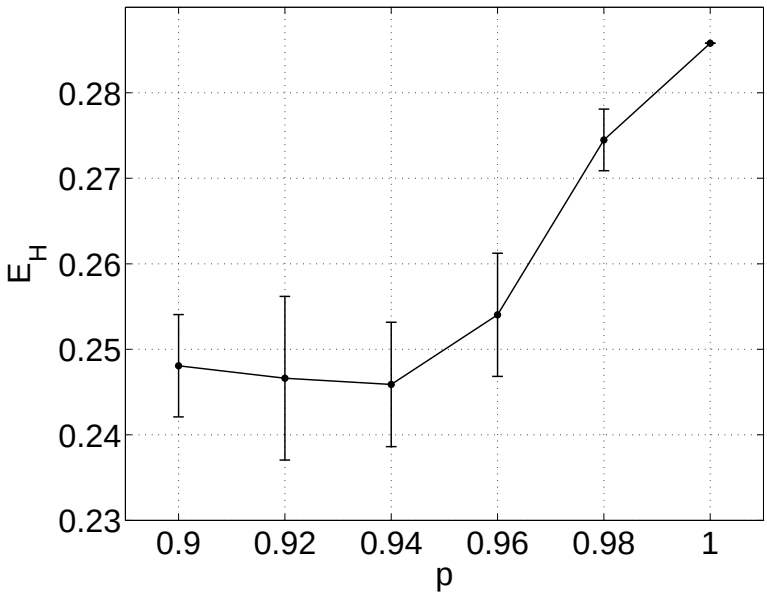

FIG. 8: Values of E at which a Hopf bifurcation of a stable stationary chimera state occurs for an Erdös-Rényi-type network, for different values of p. At each value of p, 10 realisations of the random matrices were used, and the mean and standard deviation of the 10 values of E are shown. Other parameters: $N = 300, \beta = 0.05, \Delta = 0.001$.

2. Chung-Lu-type networks

We now consider a second type of perturbation from the fully-connected case in which edges are removed preferentially so as to create a specific skewed degree distribution. The algorithm we use to create these networks is motivated by the Chung-Lu algorithm [26]. We begin by assigning to each oscillator in a subnetwork a weight $w_i = N(i/N)^r$, where $i = 1, 2, \ldots N$ is the oscillator number within the network.

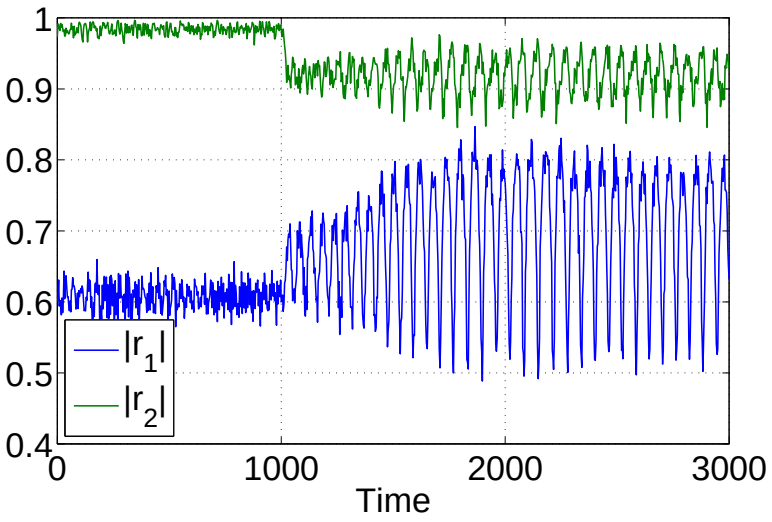

FIG. 9: Onset of a Hopf bifurcation caused by randomly removing (with equal probability) a few of the connections within the phase oscillator network (1)-(2). At $t = 1000$ we switched the connectivity matrices A, B, C and D from full to Erdös-Rényi-type matrices with $p = 0.9$. We define $r_1 = (1/N)\sum_{j=1}^{N} \exp(i\theta_j^1)$ and $r_2 = (1/N)\sum_{j=1}^{N} \exp(i\theta_j^2)$. Other parameters: $N = 300, E = 0.26, \beta = 0.05, \Delta = 0.001$.

The probability p_{ij} of the existence of a connection between oscillators i and j is given by $p_{ij} = min(q_{ij}, 1)$, where

$$q_{ij} = \frac{w_i w_j}{\sum_k w_k}. \tag{33}$$

We normalize each connectivity matrix so that the sum of all the entries of the matrix is N^2, i.e. the connections are weighted, as was the case for the Erdös-Rényi-type networks. It is easy to show that when $r = 0$ all entries of the resulting connectivity matrix equal 1, i.e. we are in the fully-connected case, and the degree distribution is effectively a delta function at N. As we increase r from zero, we obtain graphs whose degree distributions are skewed to the left (a long tail towards lower degrees). A few representative degree distributions are shown in Fig. 5 (bottom row) for r ranging between 0.01 and 0.04.

Note that in the original Chung-Lu algorithm $p_{ij} = q_{ij}$ and weights w_i are chosen such that $q_{ij} \leq 1, \forall\ (i, j)$. Here, since we allow q_{ij} to exceed 1, the weight w_i may not exactly correspond to the expected value of the degree of node i (as it does in the Chung-Lu algorithm).

Consider varying β while E is held constant at 0.2 for a Chung-Lu-type network. Doing so for various values of the parameter r and recording the value (β_{sn}) of β at which the saddle-node bifurcation occurs (c.f. Fig. 3) we obtain the results in Fig. 10. As in the Erdös-Rényi-like case, removing connections between oscillators in this way decreases the value of β at which the stable chimera state is destroyed. On the contrary, if we vary E with fixed β, for various different values of r, we obtain the results in Fig. 11. Here we see something different from the Erdös-Renyi-like case: making the matrices sparse in this way *increases* the value of E at which the Hopf bifurcation occurs (E_H). These results suggest that if we set $E = 0.3$, say, then for full connectivity we will see macroscopic oscillations, as the network has passed the Hopf bifurcation point. But for these parameters and Chung-Lu-type connectivity with r sufficiently large, a stationary chimera state is still stable. Thus if we switch connectivity from full to sparse we expect to see suppression of the oscillations, due to the Hopf bifurcation now occurring at a value of E greater than 0.3. This indeed occurs, as is demonstrated for the oscillator network (1)-(2) with Chung-Lu-type connectivity in Fig. 12. This type of simulation was repeated for a number of different realisations of the ω_i and different Chung-Lu-type connectivity matrices, and the results were always qualitatively the same.

IV. DISCUSSION

In this paper we have considered the robustness of chimera states in a particular type of network of phase oscillators with respect to randomly removing connections between oscillators in a systematic way.

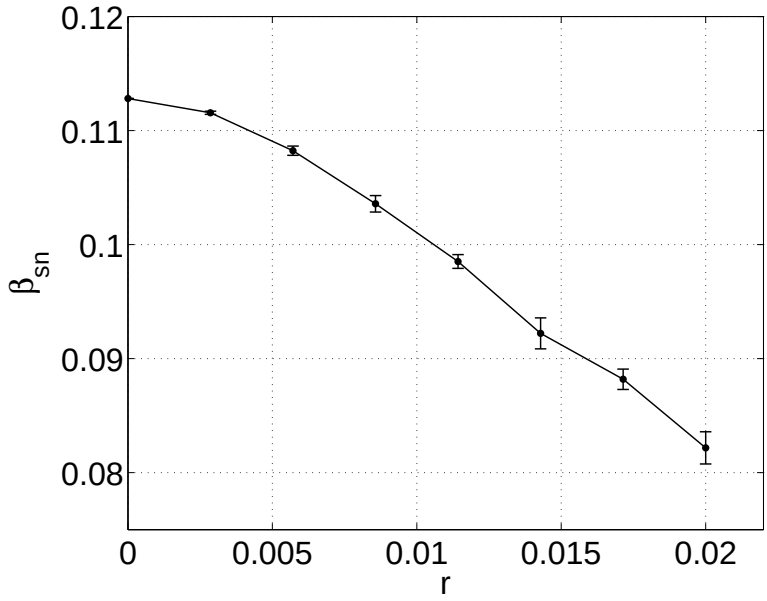

FIG. 10: The values of β_{sn} for which there is a saddle-node bifurcation of fixed points of (25)-(28) and (31)-(32) for Chung-Lu-type random matrices A, B, C and D, as a function of r. At each value of r, 10 realisations of the random matrices were used, and the mean and standard deviation of the 10 β_{sn} are shown. Other parameters: $N = 300, E = 0.2, \Delta = 0.001$.

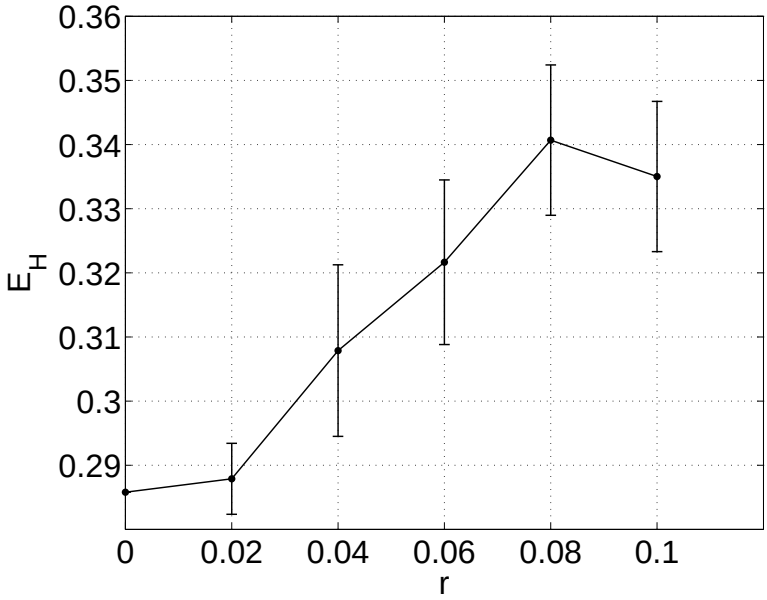

FIG. 11: Values of E at which a Hopf bifurcation of a stable stationary chimera state occurs for a Chung-Lu-type network, for different values of r. At each value of r, 10 realisations of the random matrices were used, and the mean and standard deviation of the 10 values of E are shown. Other parameters: $N = 300, \beta = 0.05, \Delta = 0.001$.

The technique we used was first presented by Barlev et al. [8], who studied the onset of synchronisation, and involves averaging over an ensemble of networks, all with the same connectivity, but with different realisations of the intrinsic frequencies of the oscillators in each member of the ensemble. This technique, combined with the ansatz of Ott and Antonsen [17–19] and an assumption that the intrinsic frequencies are chosen from a Lorentzian distribution, allowed us to derive a set of $2N$ ODEs, where N is the number of oscillators in each of the two subnetworks. Fixed points of these ODEs represent statistically stationary states of the original phase oscillator network, and these fixed points can be followed as parameters are

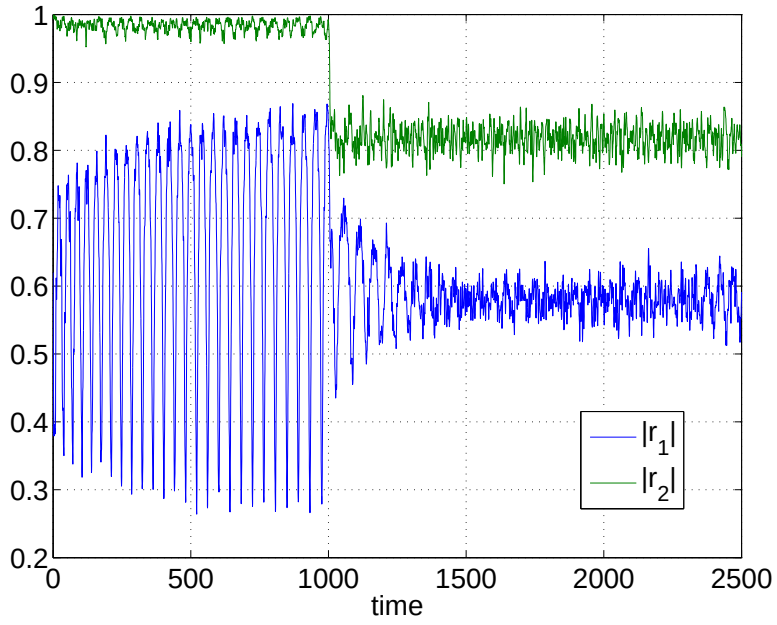

FIG. 12: Suppression of oscillations by removing some of the connections within the oscillator network (1)-(2). At $t = 1000$ we switched the connectivity matrices A, B, C and D from full to Chung-Lu-type matrices with $r = 0.1$. We define $r_1 = (1/N)\sum_{j=1}^{N} \exp(i\theta_j^1)$ and $r_2 = (1/N)\sum_{j=1}^{N} \exp(i\theta_j^2)$. Other parameters: $N = 300, E = 0.3, \beta = 0.05, \Delta = 0.001$.

varied. Thus, we can determine — on average — the effects of randomly removing connections from our network in specific ways. We chose two different parametrised families of perturbations from the fully-connected case. Firstly, we altered the probability of existence of a connection from one oscillator to another. Secondly, we removed connections in a preferential way so as to create a skewed degree distribution. We varied parameters relating to both the structure of the networks (p and r), and to the dynamics on the networks (E and β).

We found several interesting results. Firstly, these chimera states are quite sensitive to random removal of connections between oscillators. For the Erdös-Rényi-type perturbations, where we randomly remove connections with uniform probability, choosing $p = 0.93$ already has a significant effect on the range of parameter values for which a chimera state can exist (see Fig. 7). A similar statement applies for the Chung-Lu-type networks with $r = 0.02$ (see Fig. 10). This is in contrast with many results regarding the dynamics on random graphs in which transitions typically occur at much smaller values of p [27].

The second interesting result concerns the shifting of Hopf bifurcations by the removal of connections. We have considered two different perturbations from the fully connected case and found two different effects. With Erdös-Rényi-type perturbations, the Hopf bifurcation moves to lower values of E (see Fig. 8) whereas for Chung-Lu-type perturbations, the Hopf bifurcation moves to higher values of E (see Fig. 11). The implications of this are that oscillations of a chimera state via a Hopf bifurcation can be either created (Fig. 9) or destroyed (Fig. 12) by randomly removing connections (in a particular way) from within the network.

While we only considered a Lorentzian distribution of intrinsic frequencies, so that the integrals in (17)-(20) could be done explicitly, we also considered (1)-(2) when the frequencies were randomly chosen from Gaussian distributions with standard deviation 0.003 and verified that the overall trends seen in Figs. 7, 8, 10 and 11 also occurred in this case (results not shown). We have considered only two specific ways of systematically creating sparse networks by perturbing from the all-to-all coupled case, and only one type of network. Given that all-to-all connectivity with equal weights is an idealisation that is unlikely to arise in any naturally occuring network, our results are a first step towards a more general understanding of the results of the interaction between the structure *of* a network and the dynamics *on* the network.

Acknowledgements: The work of K.R. and I.G.K. was partially supported by the AFOSR and the US Department of Energy. C.R.L. was supported by the Marsden Fund Council from Government funding,

administered by the Royal Society of New Zealand.

---

[1] E. A. Martens, C. R. Laing, and S. H. Strogatz, Phys. Rev. Lett. **104**, 044101 (2010).
[2] C. R. Laing, Physica D **238**, 1569 (2009).
[3] C. R. Laing, Chaos **19**, 013113 (2009).
[4] S. Strogatz, Physica D **143**, 1 (2000).
[5] J. Acebrón, L. Bonilla, C. Pérez Vicente, F. Ritort, and R. Spigler, Rev. Mod. Phys. **77**, 137 (2005).
[6] Y. Kuramoto, *Chemical Oscillations, Waves, and Turbulence* (Springer, Berlin, 1984).
[7] D. Abrams, R. Mirollo, S. Strogatz, and D. Wiley, Phys. Rev. Lett. **101**, 084103 (2008).
[8] G. Barlev, T. M. Antonsen, and E. Ott, Chaos **21**, 025103 (2011).
[9] E. Montbrió, J. Kurths, and B. Blasius, Phys. Rev. E **70**, 056125 (2004).
[10] M. Verwoerd and O. Mason, SIAM J. Appl. Dyn. Sys. **10**, 906 (2011).
[11] D. Abrams and S. Strogatz, Phys. Rev. Lett. **93**, 174102 (2004).
[12] D. Abrams and S. Strogatz, Int. J. Bifurcat. Chaos **16**, 21 (2006).
[13] G. Sethia, A. Sen, and F. Atay, Phys. Rev. Lett. **100**, 144102 (2008).
[14] O. Omel'chenko, Y. Maistrenko, and P. Tass, Phys. Rev. Lett. **100**, 044105 (2008).
[15] E. A. Martens, Phys. Rev. E **82**, 016216 (2010).
[16] S. Shima and Y. Kuramoto, Phys. Rev. E **69**, 036213 (2004).
[17] E. Ott and T. M. Antonsen, Chaos **19**, 023117 (2009).
[18] E. Ott and T. M. Antonsen, Chaos **18**, 037113 (2008).
[19] E. Ott, B. R. Hunt, and T. M. Antonsen, Chaos **21**, 025112 (2011).
[20] A. Pikovsky and M. Rosenblum, Phys. Rev. Lett. **101**, 264103 (2008).
[21] S. Watanabe and S. Strogatz, Physica D **74**, 197 (1994).
[22] C. R. Laing, Phys. Rev. E **81**, 066221 (2010).
[23] C. Li, W. Sun, and J. Kurths, Phys. Rev. E **76**, 046204 (2007).
[24] P. So, B. Cotton, and E. Barreto, Chaos **18**, 7114 (2008).
[25] E. Barreto, B. Hunt, E. Ott, and P. So, Phys. Rev. E **77**, 036107 (2008).
[26] F. Chung and L. Lu, Annals of Combinatorics **6**, 125 (2002).
[27] T. Singh, K. Manchanda, R. Ramaswamy, and A. Bose, SIAM J. Appl. Dyn. Sys. **10**, 987 (2011).